Gamow-Teller decay of ^{142}Te to ^{142}I

B. Moon,[1,2,*] C.-B. Moon,[1,†] A. Odahara,[3] R. Lozeva,[4,5] S. Nishimura,[2] C. Yuan,[6] F. Browne,[2,7] P. Doornenbal,[2] G. Lorusso,[2] Z. Patel,[2,8] S. Rice,[2,8] L. Sinclair,[2,9] P.-A. Söderström,[10,2] T. Sumikama,[2] H. Watanabe,[2] J. Wu,[2,11] Z. Y. Xu,[12] A. Yagi,[3,2] D. S. Ahn,[1,2] H. Baba,[2] F. L. Bello Garrote,[13] R. Daido,[3,2] J. M. Daugas,[14,15] F. Didierjean,[5] Y. Fang,[3,2] N. Fukuda,[2] B. Hong,[16,17] E. Ideguchi,[18] N. Inabe,[2] T. Ishigaki,[3,2] T. Isobe,[2] H. S. Jung,[19] D. Kameda,[2] I. Kojouharov,[20] T. Komatsubara,[2] T. Kubo,[2] Y. K. Kwon,[21] C. S. Lee,[19] P. Lee,[19] S. Morimoto,[3,2] D. Murai,[22] M. Niikura,[2,12] H. Nishibata,[3,2] I. Nishizuka,[23] H. Sakurai,[2,12] Y. Shimizu,[2] H. Suzuki,[2] H. Takeda,[2] K. Tshoo,[21] and R. Yokoyama[24]

[1]*Center for Exotic Nuclear Studies, Institute for Basic Science, Daejeon 34126, Republic of Korea*
[2]*RIKEN Nishina Center, Wako, Saitama 351-0198, Japan*
[3]*Department of Physics, Osaka University, Osaka 560-0043, Japan*
[4]*Université Paris-Saclay, IJCLab, CNRS/IN2P3, F-91405 Orsay, France*
[5]*IPHC, CNRS/IN2P3 and University of Strasbourg, F-67037 Strasbourg Cedex 2, France*
[6]*Sino-French Institute of Nuclear Engineering and Technology, Sun Yat-Sen University, Zhuhai 519-082, China*
[7]*School of Computing, Engineering and Mathematics, University of Brighton BN2 4GJ, United Kingdom*
[8]*Department of Physics, University of Surrey, Guildford, GU2 7XH, United Kingdom*
[9]*Department of Physics, University of York, Heslington, York YO10 5DD, United Kingdom*
[10]*Extreme Light Infrastructure-Nuclear Physics (ELI-NP), 077125 Bucharest-Măgurele, Romania*
[11]*School of Physics and State key Laboratory of Nuclear Physics and Technology, Peking University, Beijing 100871, China*
[12]*Department of Physics, University of Tokyo, Tokyo 113-0033, Japan*
[13]*Department of Physics, University of Oslo N-0316, Norway*
[14]*Université Paris Saclay, CEA, CNRS, Inserm, SHFJ, BioMaps, 91401 Orsay, France*
[15]*CEA, DAM, DIF, F-91297 Arpajon Cedex, France*
[16]*Department of Physics, Korea University, Seoul 02841, Republic of Korea*
[17]*Center for Extreme Nuclear Matters (CENuM), Korea University, Seoul 02841, Republic of Korea*
[18]*RCNP, Osaka University, Osaka 567-0047, Japan*
[19]*Department of Physics, Chung-Ang University, Seoul 06974, Republic of Korea*
[20]*GSI Helmholtzzentrum für Schwerionenforschung GmbH, D-64291, Darmstadt, Germany*
[21]*Rare Isotope Science Project, Institute for Basic Science, Daejeon 34047, Republic of Korea*
[22]*Department of Physics, Rikkyo University, Tokyo 172-8501, Japan*
[23]*Department of Physics, Tohoku University, Sendai, Miyagi 980-8578, Japan*
[24]*Center for Nuclear Study, University of Tokyo, RIKEN Campus, Wako, Saitama 351-0198, Japan*

(Received 30 August 2022; revised 16 November 2022; accepted 11 January 2023; published 20 January 2023)

The β decay of $^{142}\mathrm{Te}_{90}$ to $^{142}\mathrm{I}_{89}$ was investigated for the first time. The parent nucleus was produced by the in-flight fission of a ^{238}U beam with an energy of 345 MeV per nucleon, impinging on a ^{9}Be target at the Radioactive Isotope Beam Factory of RIKEN. Excited states in ^{142}I were established by β-delayed γ-ray spectroscopy. The observed (1^+) states in ^{142}I could be interpreted to be predominantly the $\nu 0h_{9/2} \otimes \pi 0h_{11/2}$ configuration formed by a Gamow-Teller transition between a neutron in the $0h_{9/2}$ orbital and a proton in the $0h_{11/2}$ orbital. Additional features of the (1^+) states are discussed by comparing with neighboring heavier isotones, such as ^{144}Cs and ^{146}La. In the context of deformed shell-model calculations, the (1^+_1) state is closely related to the $\nu[5, 3, 2]3/2 \otimes \pi[5, 5, 0]1/2$ configuration, which may be related to the weak Gamow-Teller transition strength.

DOI: 10.1103/PhysRevC.107.014311

I. INTRODUCTION

In astrophysical environments, β decay of unstable nuclei plays a crucial role in generating the final isotopic abundances along with the rapid neutron-capture reaction (r process) [1–4]. The β-decay strength is largely influenced by the so-called Gamow-Teller (G-T) transition that is closely related to the spin-isospin interaction [5]. This spin-isospin excitation is one of the important ingredients for modeling the nuclear shell structure as well. Consequently, the role played by the G-T transitions provides plenty of information on both nuclear structure and nuclear astrophysics. In general, G-T response is concentrated on the G-T giant resonance region at highly excited states above 5 MeV in a daughter

*mb0316@ibs.re.kr
†cbmoon@ibs.re.kr

nucleus [6]. In contrast, low-lying G-T transitions determine abundances of isotopes produced at low temperature in the decay from the *r*-process line [7]. The G-T decay can occur between identical proton and neutron orbitals, near the $N = Z$ line, i.e., $\pi 0f_{7/2}$-$\nu 0f_{7/2}$, $\pi 0g_{9/2}$-$\nu 0g_{9/2}$, and $\pi 0h_{11/2}$-$\nu 0h_{11/2}$ or between spin-orbit partners such as $\pi 0h_{11/2}$-$\nu 0h_{9/2}$ in neutron-rich nuclei.

Investigating neutron-rich nuclei beyond the doubly magic ^{132}Sn nucleus has attracted much attention because they are expected to reveal changes in nuclear structure and contain information on nucleosynthesis along the *r*-process paths [8–19]. In this region, the only allowed G-T transition involves the transformation of a $0h_{9/2}$ neutron to a $0h_{11/2}$ proton. Such a G-T β decay of an even-even nucleus populates 1^+ states with a configuration of $\nu 0h_{9/2} \otimes \pi 0h_{11/2}$ in an odd-odd daughter nucleus [20,21]. Therefore, observing 1^+ states from the β decay of a parent nucleus provides crucial information on the evolution of single-particle states beyond ^{132}Sn, especially for $0h$ orbitals, by comparing with theoretical predictions. In this work, the level scheme of ^{142}I including newly observed (1^+) states from the β decay of ^{142}Te is established for the first time. The observed levels are discussed in the context of the deformed shell-model calculations focusing specifically on the G-T transitions.

II. EXPERIMENT AND RESULTS

The experiment was performed at the Radioactive Isotope Beam Factory (RIBF) operated by the RIKEN Nishina Center for Accelerator-Based Science and the Center for Nuclear Study of the University of Tokyo. Secondary beams were produced by the in-flight fission of a primary ^{238}U beam at 345 MeV per nucleon, impinging on a ^{9}Be target [22]. The produced rare-isotope beam was selected at the first stage of the BigRIPS spectrometer, and identified by the $B\rho$-ΔE-TOF (time-of-flight) method at the second stage of the BigRIPS and the Zero-Degree Spectrometer [23]. During the beam time, a total of 4.48×10^5 ^{142}Te ions were accumulated.

The ions were implanted on the Wide-range Active Silicon Strip Stopper Array for β and ion detection (WAS3ABi) system [24], composed of five layers of 1-mm-thick double-sided silicon strip detectors (DSSSD) with an active area of 60×40 mm^2. The implantation and decay position information was provided by 60 and 40 strips with 1-mm pitch along the x and y axis, respectively. The γ rays emitted from the implanted ions and the daughter nuclei were detected by the EUROBALL-RIKEN Cluster Array (EURICA), which consisted of 12 cluster detectors, each with seven hexagonal-tapered high-purity germanium crystals [25]. The detection efficiencies of the emitted γ rays with and without the add-back algorithm were 11.3(6)% and 8.7(4)% at 1 MeV, respectively.

Figure 1(a) represents the β-delayed γ-ray energy spectrum of ^{142}Te. The spatial correlation criterion between an implanted ion and emitted β rays in a layer of WAS3ABi was strictly constrained to the same pixel to minimize background correlations. Moreover, the timing condition, which is defined as the time difference between an implantation event and a β-decay event, was set to 0–300 ms. From this analysis,

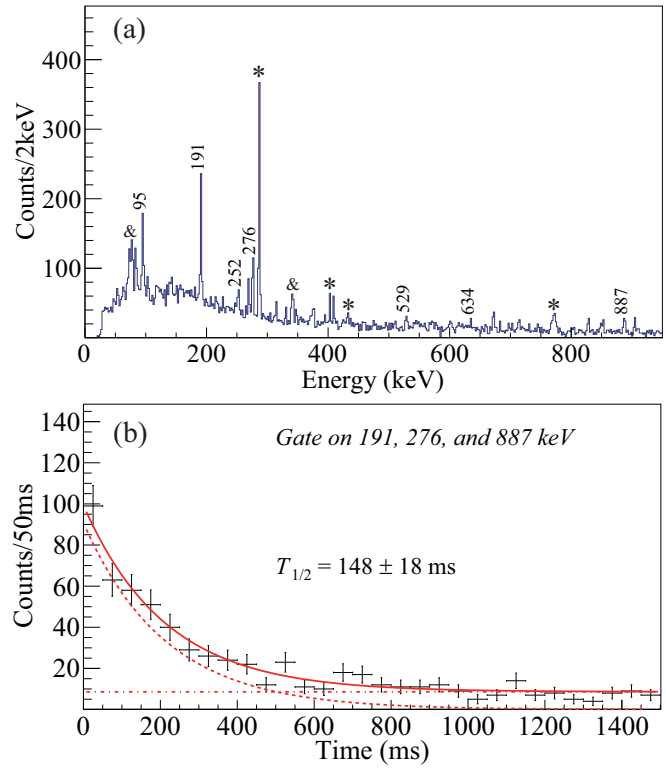

FIG. 1. (a) β-delayed γ-ray singles spectrum of ^{142}Te. The numbers represent the energies of the γ-ray transitions in ^{142}I following the β decay of ^{142}Te while background peaks in ^{142}Xe from the β decay of ^{142}I are labeled with asterisks (*). The γ-ray transitions with ampersands (&) are candidate transitions in ^{141}I from β-delayed one-neutron emission decay. (b) Half-life measurement of the ground state of ^{142}Te based on γ-transition intensities in ^{142}I as a function of time. A red solid line indicates the overall fit result including a single-component exponential decay curve (a red-dashed line) and a constant background (a red dashed-dotted line).

seven γ-ray transitions could be newly assigned to ^{142}I, as shown in Fig. 1(a). The background peaks associated with the granddaughter nucleus ^{142}Xe were also identified. The transitions with ampersands (&) are candidate transitions in ^{141}I from β-delayed one-neutron emission decay of ^{142}Te. These assignments were supported by β decays of ^{142}I and ^{141}Te in our data set, but they are beyond the scope of this paper. Two strong peaks at 409 and 672 keV were also observed. However, they could not be explicitly assigned to either ^{142}I or ^{141}I, mainly due to the experimental limitation such as the lack of γ-γ coincidence information. The half-life of the ground state of ^{142}Te was determined by gating on the 191-, 276-, and 887-keV transitions, as shown in Fig. 1(b). The decay time distribution was fitted by using the maximum-likelihood method with a fit function composed of a single-component exponential decay and a constant background. The half-life value of $T_{1/2} = 148 \pm 18$ ms was obtained, and this result is consistent with the previously measured value of 147 ± 8 ms [9].

Figure 2 contains several γ-γ coincidence results for establishing the level scheme of ^{142}I. In addition to these γ-γ

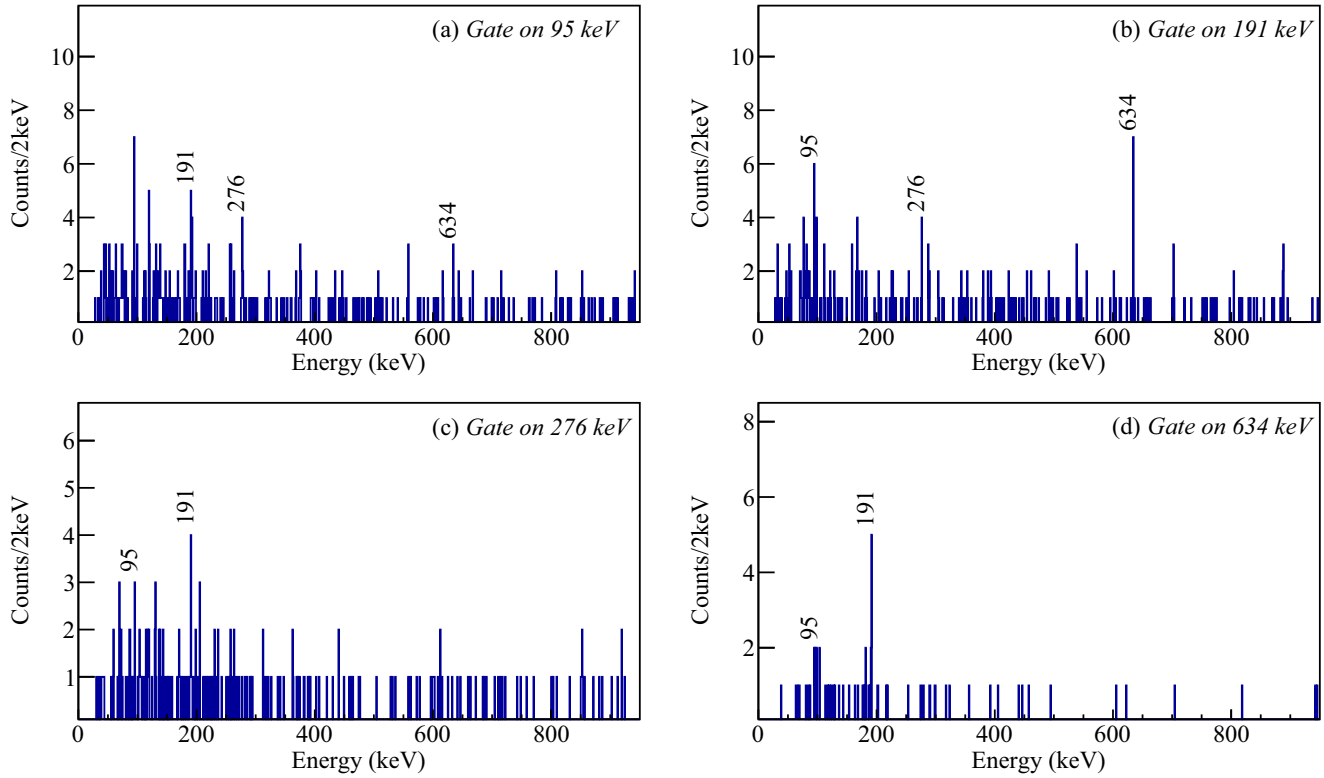

FIG. 2. γ-γ coincidence spectra of ^{142}I with gates on the (a) 95-keV, (b) 191-keV, (c) 276-keV, and (d) 634-keV transitions. The coincident transitions are indicated with their energies.

coincidence data, the γ-ray energy-sum information was also used to construct the level scheme. As a result, a level at 33.8 keV could be assigned to ^{142}I since three γ-ray transitions with energies of 252, 529, and 888 keV fit into the scheme with a same energy gap of 34 keV by deexciting the 286.1-, 562.4-, and 920.8-keV levels, respectively. Figure 3 illustrates the decay scheme of ^{142}Te observed in the present work with level information of ^{142}I such as excitation energies, spin parities, β-branching ratios, and log ft values. The experimental details of the γ-ray transitions are summarized in Table I.

The spin parity of the ground state of ^{142}I was determined by examining the levels populated in ^{142}Xe [26]. In Fig. 1(a), the $2_1^+ \rightarrow 0_1^+$ transition in ^{142}Xe with an energy of 287 keV is relatively strong, while the 403-keV transition corresponding to the $4_1^+ \rightarrow 2_1^+$ transition in ^{142}Xe is much smaller in intensity. Moreover, a similar aspect of this large difference in γ-ray intensities was also observed in the direct β-decay channel of ^{142}I to ^{142}Xe from our data set [27]. Based on the selection rule of the first-forbidden transition, the ground-state spin-parity of ^{142}I can be $(1^-, 2^-, 3^-)$. However, the (3^-) state was ruled out due to the large discrepancies in the intensities. The $4_1^+ \rightarrow 2_1^+$ transition in ^{142}Xe would be half as strong as of the $2_1^+ \rightarrow 0_1^+$ transition when the ground state of the parent nucleus has a spin parity of 3^-. The (1^-) state is also unlikely, since the 404-keV transition is still quite intense in the β-γ energy spectrum as shown in Fig. 1(a), even though it is much weaker than the 287-keV transition. Therefore, the ground-state spin and parity were assigned to be (2^-). On the other hand, the spin parities of other levels are tentatively assigned based on the log ft information [28–31]. For instance, the 286.1-keV level is proposed to have a spin parity of $(0^-, 1^-)$ based on its log ft value of 5.7(1), which may be populated by a first-forbidden transition. Although the log ft value cannot provide a clear assignment of the spin parity due to its ambiguity associated with the Pandemonium effect [32], the 562.4-keV level is a candidate for (1^+) based on its log ft value of 5.5(1) and excitation energy. Even though the log ft value is quite high for an allowed G-T transition, this assignment is supported by the systematics of the observed (1^+) states in neighboring isotopes and isotones, as shown in Fig. 4. The spin-parity assignment to the 920.8 keV level is also ambiguous. Since it has a log ft value of 5.6(1), the β transition into this level can be either an allowed G-T transition or a first-forbidden transition. Nevertheless, (1^+) is a reasonable assignment for this 920.8-keV level in terms of the energy systematics of the 1_2^+ states in I and La isotopes. For instance, the (1_2^+) levels in ^{140}I$_{87}$ and ^{146}La$_{89}$ have excitation energies of 1188.2 and 880.2 keV, respectively. However, it should be emphasized that the possibility of first-forbidden transitions to these levels cannot be ruled out.

III. DISCUSSION

Figure 4 shows the systematics of the (1_1^+) levels in $_{53}$I, $_{55}$Cs, and $_{57}$La nuclides as a function of neutron number. It is apparent that as N increases from 82, the excitation energies of the (1_1^+) levels as well as the 2_1^+ levels of neighboring even-even nuclei decrease monotonically, suggesting a

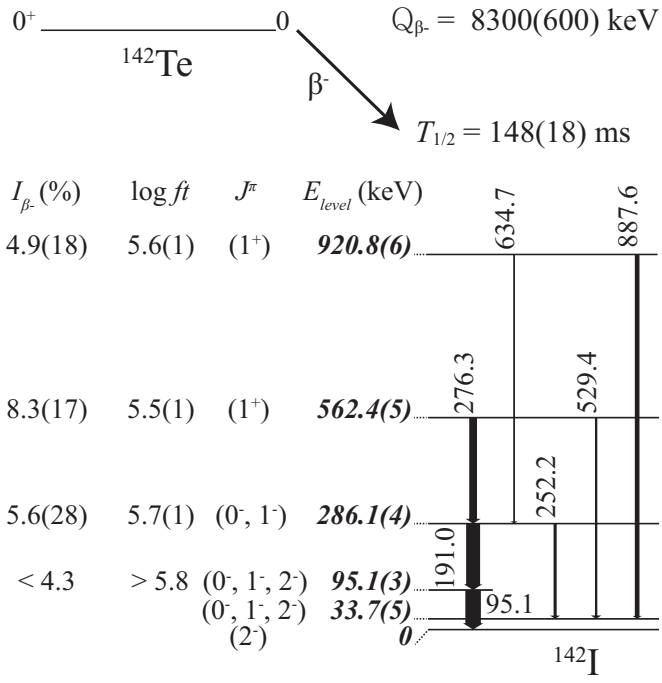

FIG. 3. β-decay scheme of ^{142}Te. The half-life of the ground state of ^{142}Te is based on the present work. The Q_{β^-} value is taken from Ref. [33]. Level information such as excitation energies, proposed spin parities, β-branching ratios, and log ft values are provided. The widths of the arrows represent relative intensities of the γ rays.

possible onset of deformation. Accordingly, the interpretation of the observed (1^+) levels in ^{142}I might be more appropriate with the deformed shell model rather than the spherical-shell model. For instance, the spherical-shell-model calculation

TABLE I. Summary of transition energies (E_γ), relative γ-ray intensities (I_γ) without and with the internal conversion electron (ICE) coefficient, and placements of γ rays observed following the β decay of ^{142}Te. The number in the parentheses is an uncertainty in the last digit. Systematic uncertainties of 0.25 keV and 5% for E_γ and I_γ, respectively, are included. The relative intensity $I_{\gamma,ICE}$ (rel.) should be multiplied by a factor of 0.11(2) to obtain the absolute intensity per 100 decays. This factor was deduced by the ratio between the 95.1-keV γ-ray events and the total β-ray events after background subtraction.

E_γ (keV)	I_γ (rel.)[a]	$I_{\gamma,ICE}$ (rel.)[a]	$E_{\text{level},i}$ (keV)	$E_{\text{level},f}$ (keV)
95.1(3)	65(21)	109(36)[b]	95.1	0
191.0(3)	100(27)	100(27)[b]	286.1	95.1
252.2(3)	21(17)	19(15)	286.1	33.8
276.3(3)	63(18)	56(16)	562.4	286.1
529.4(6)	19(12)	17(11)	562.4	33.8
634.7(4)	14(12)	12(11)	920.8	286.1
887.6(5)	36(17)	32(15)	920.8	33.8

[a]The relative γ-ray intensity, I_γ, is normalized to the intensity of the 191.0-keV transition.

[b]I_γ reported here is the total γ-ray and internal conversion intensities, calculated assuming $M1$ multipolarity.

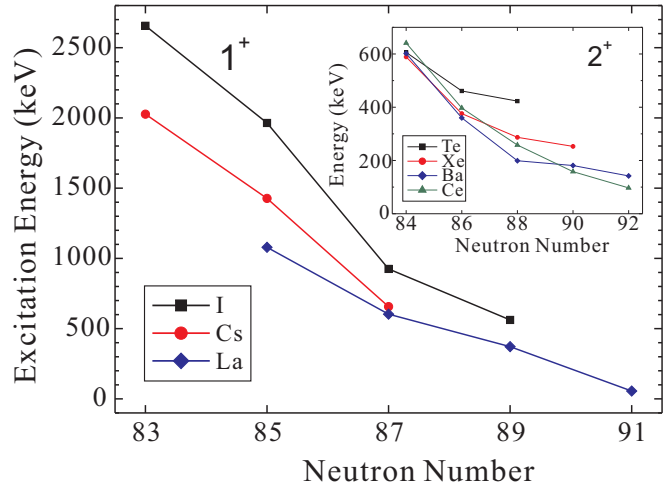

FIG. 4. Excitation energy systematics of (1_1^+) states of odd-odd I [20,21,42], Cs [43,44], and La [45–48] isotopes as a function of neutron number. The inset shows the 2_1^+ state energies for neighboring even-even Te, Xe, Ba, and Ce isotopes [26].

with the CWG interaction [34,35] predicts the first and second 1^+ states in ^{142}I associated with the $\nu 0h_{9/2} \otimes \pi 0h_{11/2}$ configuration to be located at 1381 and 1852 keV, respectively. Even higher excitation energies of 2435 and 2930 keV in ^{142}I were proposed by the KHHE interaction [36–38]. As the predicted energies of the 1^+ states are inconsistent with the present results, further discussion assuming nonzero quadrupole deformation is proposed.

For the Xe isotopes with $N = 88$ and 90, the 2_1^+ excitation energies, their energy ratios to the 4_1^+ states, $R_{4/2} = E(4_1^+)/E(2_1^+)$, and the measured 2_1^+ state lifetimes [39] suggest that their deformation magnitudes might be around $\varepsilon_2 = 0.2$. On the other hand, Te nuclei are less deformed than Xe nuclei in terms of the 2_1^+ excitation energies and $R_{4/2}$ ratios, which are representative of typical vibrators [14–16]. However, a subtle shift in terms of deformation could be observed in the odd-mass ^{139}Te$_{87}$ nucleus [40]. A rotational band structure built on the band-head $(9/2^-)$ state in this nucleus suggests a moderate deformation based on the transition energies of 535 keV $[(21/2^-) \rightarrow (17/2^-)]$, 436 keV $[(17/2^-) \rightarrow (13/2^-)]$, and 357 keV $[(13/2^-) \rightarrow (9/2^-)]$, which resembles the core excitation of the neighboring ^{140}Xe$_{86}$ nucleus with the transition energies of 582 keV $(6^+ \rightarrow 4^+)$, 458 keV $(4^+ \rightarrow 2^+)$, and 377 keV $(2^+ \rightarrow 0^+)$. Moreover, the energies of the $(17/2^-) \rightarrow (13/2^-) \rightarrow (9/2^-)$ cascading transitions at $N = 87$ are 516 and 376 keV for ^{141}Xe, and 493 and 343 keV for ^{143}Ba, respectively. It is noted that the deformation in ^{139}Te may be driven by a high-angular momentum orbital of $\nu 0h_{9/2}$ with $l = 5$. Very recently, moderate deformations of ^{142}Te and ^{144}Xe were hypothesized as $\beta_2(\varepsilon_2) = 0.18(0.17)$ and 0.20(0.18), respectively [41]. Accordingly, the excitation energies of the neutron-proton configurations in ^{142}I around the deformation parameter $\varepsilon_2 = 0.16$–0.20 are discussed in the context of the deformed shell-model calculation. The predicted excitation energies associated with the

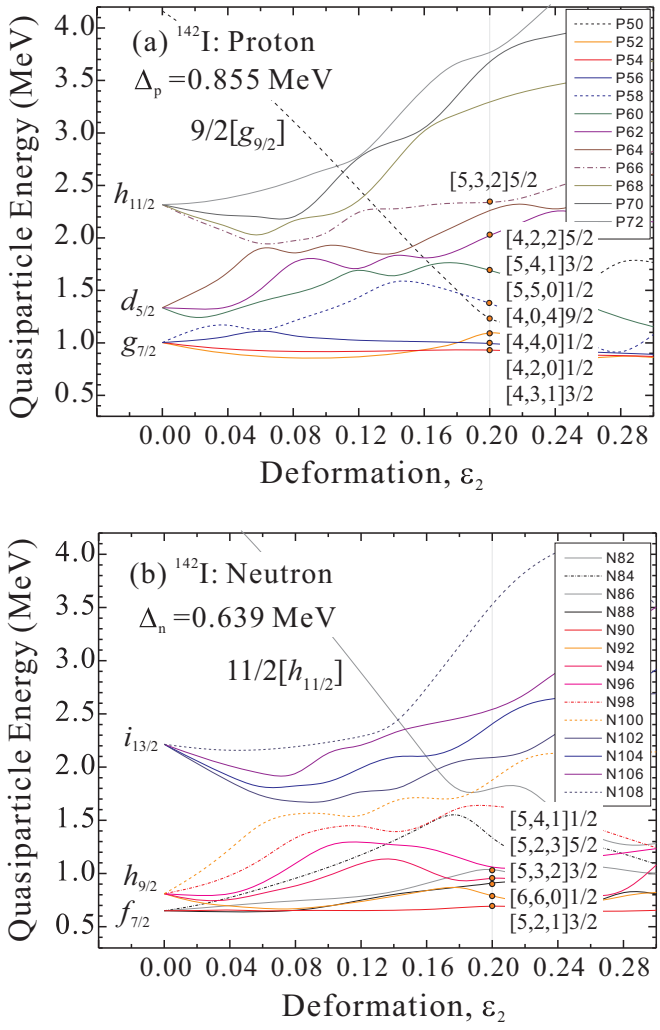

FIG. 5. Plots of the single-quasiparticle energies of (a) protons and (b) neutrons as a function of deformation parameter ε_2 for ^{142}I based on the Nilsson model. Each line follows the occupied proton or neutron number as represented in the legends. At $\varepsilon_2 = 0.20$, some low-lying orbitals are marked with the Nilsson asymptotic quantum numbers.

deformed configurations, originating from the $\nu 0h_{9/2} \otimes \pi 0h_{11/2}$ spherical-shell configuration, are inspected.

The quasiparticle energies of ^{142}I with a deformed-shell (Nilsson) model were calculated, as shown in Fig. 5 [49–51]. The Nilsson-BCS with pairing correlation calculations define a deformed quasiparticle basis with asymptotic quantum numbers, $[N, n_z, \Lambda]\Omega(= \Lambda + \Sigma)$. Here, Λ and Ω are the projections of the orbital angular momentum and the total angular momentum including the intrinsic spin (Σ), respectively. For example, the $\nu[5, 4, 1]1/2$ Nilsson orbital corresponds to the spherical-shell-based $\nu 1/2[0h_{9/2}]$ orbit. The quasiparticle energies were obtained by summing their respective energies given by $E_x = \sqrt{(E - \lambda)^2 + \Delta^2}$, where E is the single proton or neutron energy from the Hartree-Fock calculations, λ is the Fermi level, and Δ is the proton or neutron pairing strength parameter, respectively. The pairing parameters $\Delta_p = 0.855$ MeV for protons and $\Delta_n = 0.639$ MeV for neutrons, were

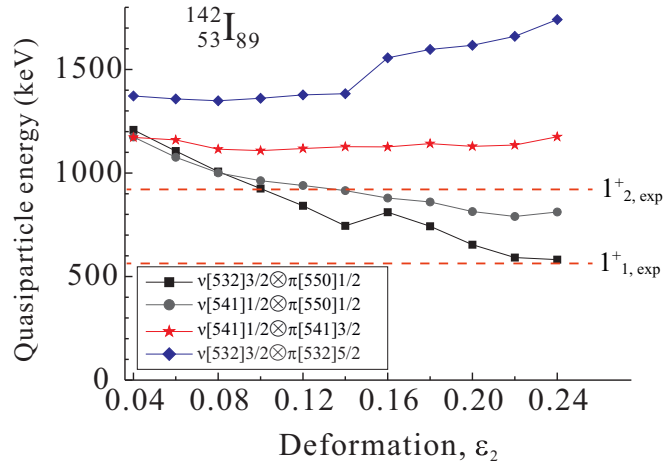

FIG. 6. Excitation energies for the components of the $\nu 0h_{9/2} \otimes \pi 0h_{11/2}$ configuration as a function of deformation for ^{142}I. The measured (1^+) excitation energies are also indicated as dashed red lines.

deduced from the recent atomic mass evaluation [33]. Several orbitals above the Fermi levels are marked by the respective Nilsson asymptotic quantum numbers. It is worth noting that the proton $\pi[5, 5, 0]1/2$, $\pi[5, 4, 1]3/2$, and $\pi[5, 3, 2]5/2$ Nilsson orbitals arise from the $\pi 0h_{112}$ orbital while the neutron $\nu[5, 3, 2]3/2$ and $\nu[5, 4, 1]1/2$ Nilsson orbitals are from the $\nu 0h_{9/2}$ orbital. The excitation energies were obtained by setting the low-lying states in Fig. 5, [4, 3, 1]3/2 for protons and [5, 2, 1]3/2 for neutrons, as to be 0.

Our results are given in Fig. 6 for the quasiparticle energies of the $\nu 0h_{9/2} \otimes \pi 0h_{11/2}$ configuration as a function of deformation parameter ε_2. One can clearly see that the lowest 1^+ state is dominated by the $\nu[5, 3, 2]3/2 \otimes \pi[5, 5, 0]1/2$ configuration from the theoretical calculations. Intriguingly, for the configurations including the $\nu[5, 3, 2]3/2$ orbital, a shape increase in energy appears between $\varepsilon_2 = 0.14$ and 0.16. This sudden increase is attributed to an interchange in the wave functions between the $\nu[5, 2, 1]3/2$ and $\nu[5, 3, 2]3/2$ orbitals, originating from the $\nu 1f_{7/2}$ and $\nu 0h_{9/2}$ orbitals, respectively. These $\nu 1f_{7/2}$ and $\nu 0h_{9/2}$ orbitals in the I isotopes with N from 88–90 are strongly admixed, and according to deformation the projection components such as $\Omega = 1/2$ and $3/2$ are interchanged. As mentioned above, as far as the excitation energies are concerned, the (1^+_1) state could be explained by a large contribution of the $\nu[5, 3, 2]3/2 \otimes \pi[5, 5, 0]1/2$ configuration at $\varepsilon_2 \approx 0.20$. As shown in Fig. 6, the lowest 1^+ level formed by this configuration is predicted at 654 keV. Moreover, the observed (1^+_2) state at the excitation energy of 921 keV may be dominated by the $\nu[5, 4, 1]1/2 \otimes \pi[5, 5, 0]1/2$ Nilsson configuration, whose energy is hypothetically 814 keV. These theoretical results at $\varepsilon_2 = 0.20$ are reasonably consistent with the experimental results in terms of the excitation energies. However, the G-T transition to the (1^+_1) state in ^{142}I with the $\nu[5, 3, 2]3/2 \otimes \pi[5, 5, 0]1/2$ configuration may be hindered due to the projection quantum number of the angular momentum difference of $\Delta\Lambda = 2$, even though the spin difference of $\Delta\Sigma = 1$ satisfies the condition of an allowed

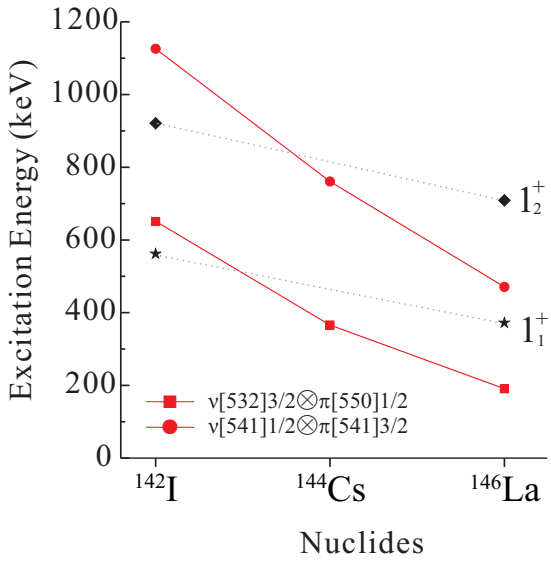

FIG. 7. Calculated excitation energies of 1^+ states associated with $\nu 0h_{9/2} \otimes \pi 0h_{11/2}$ configuration at $\varepsilon_2 = 0.2$ for I, Cs, and La with $N = 89$. For comparison, the experimental energies of the (1_1^+) and (1_2^+) states are denoted with the asterisk and diamond symbols, respectively.

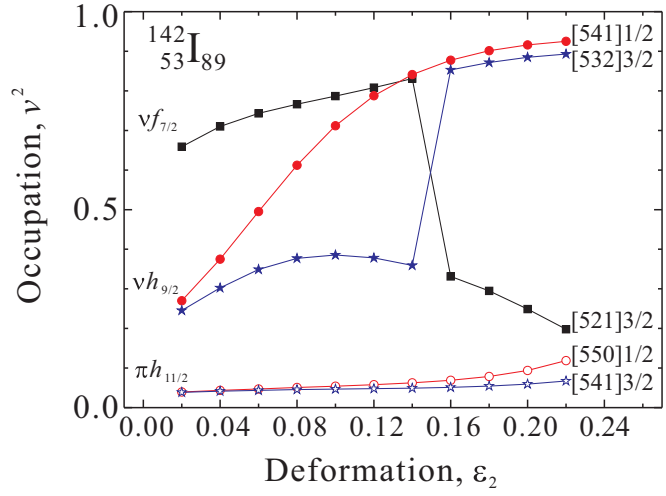

FIG. 8. Plots of occupancies for the neutron $0h_{9/2}$ and the proton $0h_{11/2}$ orbitals as a function of deformation.

G-T transition. It should be emphasized that those orbitals correspond to the $0h$ partner orbitals, thus the G-T transition is dominant when the spherical-shell basis is considered. The main reason for this hinderance is that the $\pi[5, 5, 0]1/2$ orbital cannot contribute to the optimal G-T transition since there is no spin-flip partner in the quasineutron shell, specifically the $0h_{9/2}$ orbital. On the other hand, neutron-proton interactions between the $\nu[5, 4, 1]1/2$, $\nu[5, 3, 2]3/2$, and $\nu[5, 2, 3]5/2$ orbitals and the $\pi[5, 4, 1]3/2$, $\pi[5, 3, 2]5/2$, and $\pi[5, 2, 3]7/2$ are more likely to allow G-T transitions. Therefore, the most favorable G-T transition to a 1^+ state would be the transition from a neutron in the $\nu[5, 4, 1]1/2$ orbital to a proton in the $\pi[5, 4, 1]3/2$ orbital. This is the case of an allowed transition with conditions of $\Delta\Lambda = 0$ and $\Delta\Omega = 1$. However, this $\nu[5, 4, 1]1/2 \otimes \pi[5, 4, 1]3/2$ configuration is predicted to lie at 1129 keV with $\varepsilon_2 = 0.20$ (see Fig. 6), which is far above the (1_1^+) state observed at 562 keV. Furthermore, the $\nu[5, 3, 2]3/2 \otimes \pi[5, 3, 2]5/2$ configuration which is one of the optimal G-T transition candidates is predicted at 1617 keV, which is even higher in the excitation energy. Such a Λ hindrance due to the $\pi[5, 5, 0]1/2$ Nilsson orbital might explain the relatively weak G-T transition strengths, i.e., higher log ft values of 5.5–5.6 compared to 4.5–5.0 in other deformed nuclei with a higher Z such as La [45–48]. For instance, the β decays to the (1_1^+) and (1_2^+) states in $^{144}La_{89}$ have log ft values of 4.8 and 5.1, respectively. The allowed β transitions in the well-deformed rare-earth nuclides are known to be suitable probes of a theory of G-T rates, because the single-particle Nilsson wave functions are known to be very precise [52].

Some calculated results of the 1^+ states in the $N = 89$ isotones of I, Cs, and La are plotted in Fig. 7. One is based on the $\nu[5, 3, 2]3/2 \otimes \pi[5, 5, 0]1/2$ configuration and the other one is formed by the $\nu[5, 4, 1]1/2 \otimes \pi[5, 4, 1]3/2$ configuration. From comparisons to the experimental results, two distinctive aspects appear in these three isotones. First, the predicted energies as a function of proton number decrease more drastically compared to the experimental values. This rapid decrease in the calculated excitation energies is closely related to the proton $0h_{11/2}$ orbital, because the Fermi surface leads to lower excitation energies for the $\pi[5, 5, 0]1/2$ or $\pi 1/2[0h_{11/2}]$ component as Z increases from 53–57. Second, the (1_1^+) state in ^{146}La is close to the $\nu[5, 4, 1]1/2 \otimes \pi[5, 4, 1]3/2$ configuration with optimal conditions of the G-T transition while for ^{142}I it is located near the $\nu[5, 3, 2]3/2 \otimes \pi[5, 5, 0]1/2$ configuration. Despite the absence of experimental data for ^{144}Cs, the 1_1^+ state might be inferred to be associated with the $\nu[5, 3, 2]3/2 \otimes \pi[5, 5, 0]1/2$ configuration. Therefore, the weak G-T transition strengths for ^{142}I are attributed to the $\pi[5, 5, 0]1/2$ orbital while for ^{146}La the G-T transitions are thoroughly induced by the $\nu[5, 4, 1]1/2$ and the $\pi[5, 4, 1]3/2$ orbitals, giving rise to the strong transition strengths.

The G-T transition amplitude is proportional to the occupation (v) and vacancy (u) ($v^2 + u^2 = 1$) coefficients, specifically $v_n u_p$ for creating one quasineutron in the $[N, n_z, \Lambda]\Omega(= \Lambda - 1/2)$ orbital and one quasiproton in the $[N, n_z, \Lambda]\Omega(= \Lambda + 1/2)$ orbital [7]. Therefore, a strong G-T strength is likely due to high occupation of the $\nu[5, 4, 1]1/2$ and $\nu[5, 3, 2]3/2$ orbitals, while the $\pi[5, 4, 1]3/2$ and $\pi[5, 5, 0]1/2$ orbitals would be relatively empty. Figure 8 shows the occupancy distributions of the Nilsson orbitals of interest as a function of deformation. For $\varepsilon_2 \geqslant 0.16$, the $\nu[5, 4, 1]1/2$ and $[5, 3, 2]3/2$ orbitals are surely occupied with $v^2 = 0.85$–0.9, while the $\pi[5, 5, 0]1/2$ and $[5, 4, 1]3/2$ orbitals are almost empty as $v^2 \leqslant 0.1$. However, at $\varepsilon_2 = 0.20$, the occupation of the $[5, 5, 0]1/2$ orbital is not negligible. Then a weaker probability for the G-T transition is anticipated as this orbital is filled. In summary, the number of nucleons and deformation in ^{142}I lead to a strong contribution of the $\pi[5, 5, 0]1/2$ Nilsson orbital originating from the $\pi 0h_{11/2}$ spherical-shell

TABLE II. The calculated excitation energies, E_x and occupation probabilities, $v_n u_p$ for the neutron-proton configurations responsible for Gamow-Teller transitions from ^{142}Te to ^{142}I when deformations are $\varepsilon_2 = 0.20$.

Configuration	E_x (keV)	$v_n u_p$
$\nu[5,3,2]3/2 \otimes \pi[5,5,0]1/2$	654	0.81
$\nu[5,4,1]1/2 \otimes \pi[5,5,0]1/2$	814	0.85
$\nu[5,4,1]1/2 \otimes \pi[5,4,1]3/2$	1129	0.94
$\nu[5,3,2]3/2 \otimes \pi[5,3,2]5/2$	1617	0.91

orbital. This effect leads to a hindered, weak G-T transition strength due to the absence of the spin-flip partner Nilsson orbital. In Table II, the excitation energies and the occupation probabilities for the neutron-proton configurations leading to the G-T transitions are summarized.

IV. CONCLUSION

In the present work, an experimental β-decay scheme of ^{142}Te to ^{142}I was observed for the first time. Two levels at 562 and 921 keV were suggested to be (1^+) states by assessing their log ft values. Our assignments were consistent with the energy systematics of the Cs and La isotones. In order to investigate the observed levels, a deformed shell-model approach was adopted instead of a spherical-shell model due to the moderate quadrupole deformation of ^{142}I. The observed (1^+) states could be interpreted as a manifestation of the $\nu 0h_{9/2} \otimes \pi 0h_{11/2}$ configuration related to the G-T transition between a neutron in the $\nu 0h_{9/2}$ orbital and a proton in the $\pi 0h_{11/2}$ orbital. By considering the excitation energy and occupation factors, these (1^+) states were suggested to possess a dominant $\pi[5,5,0]1/2$ Nilsson orbital component due to circumstantial evidence such as the number of nucleons and the assumed deformation parameter $\varepsilon_2 = 0.20$. Upon detailed scrutiny of various theoretical results, this $\pi[5,5,0]1/2$ Nilsson orbital may be the reason for the weak G-T transition strengths observed in ^{142}I due to the absence of the spin-flip partner orbital on the quasineutron side.

ACKNOWLEDGMENTS

This work was carried out at the RIBF operated by RIKEN Nishina Center and CNS, University of Tokyo. We acknowledge the EUROBALL Owners Committee for the loan of germanium detectors and the PreSpec Collaboration for the readout electronics of the cluster detectors. Part of the WAS3ABi was supported by the Rare Isotope Science Project (RISP) of the Institute for Basic Science (IBS) funded by the Ministry of Science, ICT and Future Planning (MSIP) and National Research Foundation (NRF) of the Republic of Korea (Grant No. 2013M7A1A1075764). This research was supported by IBS of the Republic of Korea (Grants No. IBS-R031-D1 and No. IBS-R031-Y1), NRF of the Republic of Korea (Grants No. 2019R1A6A3A03031564 and No. 2018R1A5A1025563), and JSPS KAKENHI of Japan (Grant No. 25247045). The support from FR-JP LIA is also acknowledged. C.S.L. acknowledges the support from NRF of the Republic of Korea (Grants No. 2017M2A2A6A02071071 and No. 2016R1D1A1A09917463). C.Y. acknowledges the support from the National Natural Science Foundation of China under Grant No. 11775316. We thank J. Park at CENS, IBS for his kind English proofreading.

[1] J. J. Cowan, F.-K. Thielemann, and J. W. Truran, Phys. Rep. **208**, 267 (1991).
[2] M. Mumpower, R. Suman, D. L. Fang, M. Beard, and A. Aprahama, J. Phys. G: Nucl. Part. Phys. **42**, 034027 (2015).
[3] K.-L. Kratz, B. Pfeiffer, and F.-K. Thielemann, Nucl. Phys. A **630**, 352 (1998).
[4] M. Arnould, S. Goriely, and K. Takahashi, Phys. Rep. **450**, 97 (2007).
[5] K. Langanke and G. Martínez-Pinedo, Rev. Mod. Phys. **75**, 819 (2003).
[6] B. L. Berman and S. C. Fultz, Rev. Mod. Phys. **47**, 713 (1975).
[7] P. Urkedal, X. Z. Zhang, and I. Hamamoto, Phys. Rev. C **64**, 054304 (2001).
[8] K.-L. Kratz, B. Pfeiffer, O. Arndt, S. Hennrich, and A. Wöhr, Eur. Phys. J. A **25**, 633 (2005).
[9] J. Wu, S. Nishimura, P. Möller, M. R. Mumpower, R. Lozeva, C. B. Moon, A. Odahara, H. Baba, F. Browne, R. Daido, P. Doornenbal, Y. F. Fang, M. Haroon, T. Isobe, H. S. Jung, G. Lorusso, B. Moon, Z. Patel, S. Rice, H. Sakurai, Y. Shimizu, L. Sinclair, P.-A. Söderström, T. Sumikama, H. Watanabe, Z. Y. Xu, A. Yagi, R. Yokoyama, D. S. Ahn, F. L. Bello Garrote, J. M. Daugas, F. Didierjean, N. Fukuda, N. Inabe, T. Ishigaki, D. Kameda, I. Kojouharov, T. Komatsubara, T. Kubo, N. Kurz, K. Y. Kwon, S. Morimoto, D. Murai, H. Nishibata, H. Schaffner, T. M. Sprouse, H. Suzuki, H. Takeda, M. Tanaka, K. Tshoo, and Y. Wakabayashi, Phys. Rev. C **101**, 042801(R) (2020).
[10] K. L. Jones, A. S. Adekola, D. W. Bardayan, J. C. Blackmon, K. Y. Chae, K. A. Chipps, J. A. Cizewski, L. Erikson, C. Harlin, R. Hatarik, R. Kapler, R. L. Kozub, J. F. Liang, R. Livesay, Z. Ma, B. H. Moazen, C. D. Nesaraja, F. M. Nunes, S. D. Pain, N. P. Patterson, D. Shapira, J. F. Shriner Jr., M. S. Smith, T. P. Swan, and J. S. Thomas, Nature (London) **465**, 454 (2010).
[11] D. C. Radford, C. Baktash, J. R. Beene, B. Fuentes, A. Galindo-Uribarri, C. J. Gross, P. A. Hausladen, T. A. Lewis, P. E. Mueller, E. Padilla, D. Shapira, D. W. Stracener, C.-H. Yu, C. J. Barton, M. A. Caprio, L. Coraggio, A. Covello, A. Gargano, D. J. Hartley, and N. V. Zamfir, Phys. Rev. Lett. **88**, 222501 (2002).
[12] J. M. Allmond, A. E. Stuchbery, C. Baktash, A. Gargano, A. Galindo-Uribarri, D. C. Radford, C. R. Bingham, B. A. Brown, L. Coraggio, A. Covello, M. Danchev, C. J. Gross, P. A. Hausladen, N. Itaco, K. Lagergren, E. Padilla-Rodal, J. Pavan, M. A. Riley, N. J. Stone, D. W. Stracener, R. L. Varner, and C.-H. Yu, Phys. Rev. Lett. **118**, 092503 (2017).
[13] V. Vaquero, A. Jungclaus, P. Doornenbal, K. Wimmer, A. M. Moro, K. Ogata, T. Furumoto, S. Chen, E. Nácher, E. Sahin,

Y. Shiga, D. Steppenbeck, R. Taniuchi, Z. Y. Xu, T. Ando, H. Baba, F. L. Bello Garrote, S. Franchoo, K. Hadynska-Klek, A. Kusoglu, J. Liu, T. Lokotko, S. Momiyama, T. Motobayashi, S. Nagamine, N. Nakatsuka, M. Niikura, R. Orlandi, T. Y. Saito, H. Sakurai, P. A. Söderström, G. M. Tveten, Z. Vajta, and M. Yalcinkaya, Phys. Rev. C **99**, 034306 (2019).

[14] P. Lee, C.-B. Moon, C. S. Lee, A. Odahara, R. Lozeva, A. Yagi, S. Nishimura, P. Doornenbal, G. Lorusso, P.-A. Söderström, T. Sumikama, H. Watanabe, T. Isobe, H. Baba, H. Sakurai, F. Browne, R. Daido, Y. Fang, H. Nishibata, Z. Patel, S. Rice, L. Sinclair, J. Wu, Z. Y. Xu, R. Yokoyama, T. Kubo, N. Inabe, H. Suzuki, N. Fukuda, D. Kameda, H. Takeda, D. S. Ahn, D. Murai, F. L. B. Garrote, J. M. Daugas, F. Didierjean, E. Ideguchi, T. Ishigaki, H. S. Jung, T. Komatsubara, Y. K. Kwon, S. Morimoto, M. Niikura, I. Nishizuka, and K. Tshoo, Phys. Rev. C **92**, 044320 (2015).

[15] B. Moon, C.-B. Moon, P.-A. Söderström, A. Odahara, R. Lozeva, B. Hong, F. Browne, H. S. Jung, P. Lee, C. S. Lee, A. Yagi, C. Yuan, S. Nishimura, P. Doornenbal, G. Lorusso, T. Sumikama, H. Watanabe, I. Kojouharov, T. Isobe, H. Baba, H. Sakurai, R. Daido, Y. Fang, H. Nishibata, Z. Patel, S. Rice, L. Sinclair, J. Wu, Z. Y. Xu, R. Yokoyama, T. Kubo, N. Inabe, H. Suzuki, N. Fukuda, D. Kameda, H. Takeda, D. S. Ahn, Y. Shimizu, D. Murai, F. L. Bello Garrote, J. M. Daugas, F. Didierjean, E. Ideguchi, T. Ishigaki, S. Morimoto, M. Niikura, I. Nishizuka, T. Komatsubara, Y. K. Kwon, and K. Tshoo, Phys. Rev. C **95**, 044322 (2017).

[16] B. Moon, A. Jungclaus, H. Naïdja, A. Gargano, R. Lozeva, C.-B. Moon, A. Odahara, G. S. Simpson, S. Nishimura, F. Browne, P. Doornenbal, G. Gey, J. Keatings, G. Lorusso, Z. Patel, S. Rice, M. Si, L. Sinclair, P.-A. Söderström, T. Sumikama, J. Taprogge, H. Watanabe, J. Wu, Z. Y. Xu, A. Yagi, D. S. Ahn, H. Baba, F. L. Bello Garrote, S. Bönig, R. Daido, J. M. Daugas, F. Didierjean, F. Drouet, Y. Fang, N. Fukuda, R. Gernhäuser, B. Hong, E. Ideguchi, S. Ilieva, N. Inabe, T. Ishigaki, T. Isobe, H. S. Jung, D. Kameda, I. Kojouharov, T. Komatsubara, T. Kröll, T. Kubo, N. Kurz, Y. K. Kwon, C. S. Lee, P. Lee, Z. Li, A. Montaner-Pizá, S. Morimoto, K. Moschner, D. Mücher, D. Murai, M. Niikura, H. Nishibata, I. Nishizuka, R. Orlandi, H. Sakurai, H. Schaffner, Y. Shimizu, K. Steiger, H. Suzuki, H. Takeda, K. Tshoo, Z. Vajta, A. Wendt, R. Yokoyama, and K. Yoshinaga, Phys. Rev. C **103**, 034320 (2021).

[17] G. S. Simpson, G. Gey, A. Jungclaus, J. Taprogge, S. Nishimura, K. Sieja, P. Doornenbal, G. Lorusso, P.-A. Söderström, T. Sumikama, Z. Y. Xu, H. Baba, F. Browne, N. Fukuda, N. Inabe, T. Isobe, H. S. Jung, D. Kameda, G. D. Kim, Y.-K. Kim, I. Kojouharov, T. Kubo, N. Kurz, Y. K. Kwon, Z. Li, H. Sakurai, H. Schaffner, Y. Shimizu, H. Suzuki, H. Takeda, Z. Vajta, H. Watanabe, J. Wu, A. Yagi, K. Yoshinaga, S. Bönig, J.-M. Daugas, F. Drouet, R. Gernhäuser, S. Ilieva, T. Kröll, A. Montaner-Pizá, K. Moschner, D. Mücher, H. Naïdja, H. Nishibata, F. Nowacki, A. Odahara, R. Orlandi, K. Steiger, and A. Wendt, Phys. Rev. Lett. **113**, 132502 (2014).

[18] A. Jungclaus, J. M. Keatings, G. S. Simpson, H. Naïdja, A. Gargano, S. Nishimura, P. Doornenbal, G. Gey, G. Lorusso, P.-A. Söderström, T. Sumikama, J. Taprogge, Z. Y. Xu, H. Baba, F. Browne, N. Fukuda, N. Inabe, T. Isobe, H. S. Jung, D. Kameda, G. D. Kim, Y.-K. Kim, I. Kojouharov, T. Kubo, N. Kurz, Y. K. Kwon, Z. Li, H. Sakurai, H. Schaffner, Y. Shimizu, H. Suzuki, H. Takeda, Z. Vajta, H. Watanabe, J. Wu, A. Yagi, K. Yoshinaga, S. Bönig, J.-M. Daugas, R. Gernhäuser, S. Ilieva, T. Kröll, A. Montaner-Piza, K. Moschner, D. Mücher, H. Nishibata, A. Odahara, R. Orlandi, M. Scheck, K. Steiger, and A. Wendt, Phys. Rev. C **102**, 034324 (2020).

[19] R. Lozeva, H. Naïdja, F. Nowacki, J. Dudek, A. Odahara, C.-B. Moon, S. Nishimura, P. Doornenbal, J.-M. Daugas, P.-A. Söderström, T. Sumikama, G. Lorusso, J. Wu, Z. Y. Xu, H. Baba, F. Browne, R. Daido, Y. Fang, T. Isobe, I. Kojouharov, N. Kurz, Z. Patel, S. Rice, H. Sakurai, H. Schaffner, L. Sinclair, H. Watanabe, A. Yagi, R. Yokoyama, T. Kubo, N. Inabe, H. Suzuki, N. Fukuda, D. Kameda, H. Takeda, D. S. Ahn, D. Murai, F. L. Bello Garrote, F. Didierjean, E. Ideguchi, T. Ishigaki, H. S. Jung, T. Komatsubara, Y. K. Kwon, P. Lee, C. S. Lee, S. Morimoto, M. Niikura, H. Nishibata, and I. Nishizuka, Phys. Rev. C **93**, 014316 (2016).

[20] B. Moon, C.-B. Moon, A. Odahara, R. Lozeva, P.-A. Söderström, F. Browne, C. Yuan, A. Yagi, B. Hong, H. S. Jung, P. Lee, C. S. Lee, S. Nishimura, P. Doornenbal, G. Lorusso, T. Sumikama, H. Watanabe, I. Kojouharov, T. Isobe, H. Baba, H. Sakurai, R. Daido, Y. Fang, H. Nishibata, Z. Patel, S. Rice, L. Sinclair, J. Wu, Z. Y. Xu, R. Yokoyama, T. Kubo, N. Inabe, H. Suzuki, N. Fukuda, D. Kameda, H. Takeda, D. S. Ahn, Y. Shimizu, D. Murai, F. L. Bello Garrote, J. M. Daugas, F. Didierjean, E. Ideguchi, T. Ishigaki, S. Morimoto, M. Niikura, I. Nishizuka, T. Komatsubara, Y. K. Kwon, and K. Tshoo, Phys. Rev. C **96**, 014325 (2017).

[21] B. Moon, A. Gargano, H. Naïdja, C.-B. Moon, A. Odahara, R. Lozeva, S. Nishimura, C. Yuan, F. Browne, P. Doornenbal, G. Lorusso, Z. Patel, S. Rice, M. Si, L. Sinclair, P.-A. Söderström, T. Sumikama, H. Watanabe, J. Wu, Z. Y. Xu, A. Yagi, D. S. Ahn, H. Baba, F. L. Bello Garrote, R. Daido, J. M. Daugas, F. Didierjean, Y. Fang, N. Fukuda, B. Hong, E. Ideguchi, N. Inabe, T. Ishigaki, T. Isobe, H. S. Jung, D. Kameda, I. Kojouharov, T. Komatsubara, T. Kubo, Y. K. Kwon, C. S. Lee, P. Lee, S. Morimoto, D. Murai, M. Niikura, H. Nishibata, I. Nishizuka, H. Sakurai, Y. Shimizu, H. Takeda, K. Tshoo, and R. Yokotama, Phys. Rev. C **105**, 034334 (2022).

[22] T. Kubo, D. Kameda, H. Suzuki, N. Fukuda, H. Takeda, Y. Yanagisawa, M. Ohtake, K. Kusaka, K. Yoshida, N. Inabe, T. Ohnishi, A. Yoshida, K. Tanaka, and Y. Mizoi, Prog. Theor. Exp. Phys. **2012**, 03C003 (2012).

[23] N. Fukuda, T. Kubo, T. Ohnishi, N. Inabe, H. Takeda, D. Kameda, and H. Suzuki, Nucl. Instrum. Meth. Phys. Res. B **317**, 323 (2013).

[24] S. Nishimura, Prog. Theor. Exp. Phys. **2012**, 03C006 (2012).

[25] P.-A. Söderström, S. Nishimura, P. Doornenbal, G. Lorusso, T. Sumikama, H. Watanabe, Z. Y. Xu, H. Baba, F. Browne, S. Go, G. Gey, T. Isobe, H.-S. Jung, G. D. Kim, Y.-K. Kim, I. Kojouharov, N. Kurz, Y. K. Kwon, Z. Li, K. Moschner, T. Nakao, H. Nishibata, M. Nishimura, A. Odahara, H. Sakurai, H. Schaffner, T. Shimoda, J. Taprogge, Zs. Vajta, V. Werner, J. Wu, A. Yagi, and K. Yoshinaga, Nucl. Instrum. Meth. Phys. Res. B **317**, 649 (2013).

[26] National Nuclear Data Center, Brookhaven National Laboratory, http://www.nndc.bnl.gov.

[27] A. Odahara *et al.* (in private communication).

[28] B. Singh, J. L. Rodriguez, S. S. M. Wong, and J. K. Tuli, Nucl. Data Sheets **84**, 487 (1998).

[29] H. Abele, M. A. Hoffmann, S. Baeßler, D. Dubbers, F. Glück, U. Müller, V. Nesvizhevsky, J. Reich, and O. Zimmer, Phys. Rev. Lett. **88**, 211801 (2002).

[30] B. Rubio, W. Gelletly, E. Nácher, A. Algora, J. L. Taín, A. Pérez, and L. Caballero, J. Phys. G: Nucl. Part. Phys. **31**, S1477 (2005).
[31] S. Raman and N. B. Gove, Phys. Rev. C **7**, 1995 (1973).
[32] J. Hardy, L. C. Carraz, B. Jonson, and P. G. Hansen, Phys. Lett. B **71**, 307 (1977).
[33] M. Wang, W. J. Huang, F. G. Condev, G. Audi, and S. Naimi, Chin. Phys. C **45**, 030003 (2021).
[34] W.-T. Chou and E. K. Warburton, Phys. Rev. C **45**, 1720 (1992).
[35] B. A. Brown, N. J. Stone, J. R. Stone, I. S. Towner, and M. Hjorth-Jensen, Phys. Rev. C **71**, 044317 (2005).
[36] E. K. Warburton and B. A. Brown, Phys. Rev. C **43**, 602 (1991).
[37] L. Rydström, J. Blomqvist, R. J. Liotta, and C. Pomar, Nucl. Phys. A **512**, 217 (1990).
[38] J. B. McGrory and T. T. S. Kuo, Nucl. Phys. A **247**, 283 (1975).
[39] S. Ilieva, T. Kröll, J.-M. Régis, N. Saed-Samii, A. Blanc, A. M. Bruce, L. M. Fraile, G. de France, A.-L. Hartig, C. Henrich, A. Ignatov, M. Jentschel, J. Jolie, W. Korten, U. Köster, S. Lalkovski, R. Lozeva, H. Mach, N. Marginean, P. Mutti, V. Paziy, P. H. Regan, G. S. Simpson, T. Soldner, M. Thürauf, C. A. Ur, W. Urban, and N. Warr, Phys. Rev. C **94**, 034302 (2016).
[40] W. Urban, W. R. Phillips, N. Schulz, B. J. P. Gall, I. Ahmad, M. Bentaleb, J. L. Durell, M. A. Jones, M. J. Leddy, E. Lubkiewicz, L. R. Morss, A. G. Smith, and B. J. Varley, Phys. Rev. C **62**, 044315 (2000).
[41] K. Zhang *et al.*, At. Data Nucl. Data Tables **144**, 101488 (2022).
[42] F. Schussler, J. Blachot, E. Monnand, J. A. Pinston, B. Pfeiffer, K. Hawerkamp, and R. Stippler, Z. Phys. A **283**, 43 (1977).
[43] G. H. Carlson, W. L. Talbert Jr., and J. R. McConnell, Phys. Rev. C **9**, 283 (1974).
[44] D. Otero, A. N. Proto, E. Duering, and M. L. Perez, Phys. Rev. C **23**, 2691 (1981).
[45] C. Chung, W. B. Walters, D. S. Brenner, A. Aprahamian, R. L. Gill, M. Shmid, R. E. Chrien, L.-J. Yuan, A. Wolf, and Z. Berant, Phys. Rev. C **28**, 2099 (1983).
[46] C. Chung, W. B. Walters, R. L. Gill, M. Shmid, R. E. Chrien, and D. S. Brenner, Phys. Rev. C **26**, 1198 (1982).
[47] C. Chung, W. B. Walters, D. S. Brenner, R. L. Gill, M. Shmid, Y. Y. Chu, R. E. Chrien, L.-J. Yuan, F. K. Wohn, and R. A. Meyer, Phys. Rev. C **31**, 2199 (1985).
[48] C. Chung, W. B. Walters, N. K. Aras, F. K. Wohn, D. S. Brenner, Y. Y. Chu, M. Shmid, R. L. Gill, R. E. Chrien, and L.-J. Yuan, Phys. Rev. C **29**, 592 (1984).
[49] S. G. Nilsson *et al.*, Nucl. Phys. A **131**, 1 (1969).
[50] Y. R. Shimizu and K. Matsuyanagi, Prog. Theor. Phys. **71**, 960 (1984).
[51] Y. R. Shimizu and K. Matsuyanagi, Prog. Theor. Phys. **74**, 1346 (1985).
[52] A. K. Jain, R. K. Sheline, D. M. Headly, P. C. Sood, D. G. Burke, I. Hrivnacova, J. Kvasil, D. Nosek, and R. W. Hoff, Rev. Mod. Phys. **70**, 843 (1998).